

Supplementary Material

Table S1. Statistical parameters derived from the linear fitting of the graphs reported in Figure 2 by considering β -sheet and α -helix structures separately. For parameters with $R < 0.70$ the p-value has been calculated and reported in bracket.

Parameter	β -sheet		α -helix	
	Correlation coefficient R	Regression line	Correlation coefficient R	Regression line
NC ^{α} C	0.88	y=0.81x+21.1	0.89	y=0.49x+57.7
NC ^{α} C ^{β}	0.76	y=0.78x+24.7	0.25 (0.0055)	y=0.25x+83.2
C ^{β} C ^{α} C	0.93	y=0.84x+17.8	0.80	y=0.59x+44.7
C ^{α} CO	0.87	y=0.80x+24.3	0.89	y=0.66x+41.0
C ^{α} CN ⁺¹	0.84	y=0.69x+36.2	0.82	y=0.82x+21.1
OCN ⁺¹	0.72	y=0.63x+45.9	0.10 (0.25)	y=0.076x+113.5
C ⁻¹ NC ^{α}	0.78	y=0.71x+35.5	0.76	y=0.75x+30.9
$\Delta\omega$	0.92	y=0.87x+0.92	0.71	y=0.41x+1.2
θ_C	0.94	y=0.85x-0.15	0.77	y=0.62x+0.68

Table S2. Engl and Huber parameters for different backbone dihedral angles. The number reported in the second row is the standard deviation.

Angle	NC ^{α} C	C ^{α} CO	C ^{α} CN ⁺¹	OCN ⁺¹	C ⁻¹ NC ^{α}	NC ^{α} C ^{β}	C ^{β} C ^{α} C
Residue							
Pro	111.8 2.5	-	116.9 1.5	122.0 1.4	122.6 5.0	103.0 1.1	-
Non-Pro	-	-	-	123.0 1.6	-	-	-
Gly	112.5 2.9	120.8 2.1	116.4 2.1	-	120.6 1.7	-	-
Non-Gly	-	120.8 1.7	-	-	-	-	-
Ala	-	-	-	-	-	110.4 1.5	110.5 1.5
Ile, Thr, Val	-	-	-	-	-	111.5 1.7	109.1 2.2
Non-Gly/non-Pro	111.2 2.8	-	116.2 2.0	-	121.7 1.8	-	-
The rest	-	-	-		-	110.5 1.7	110.1 1.9

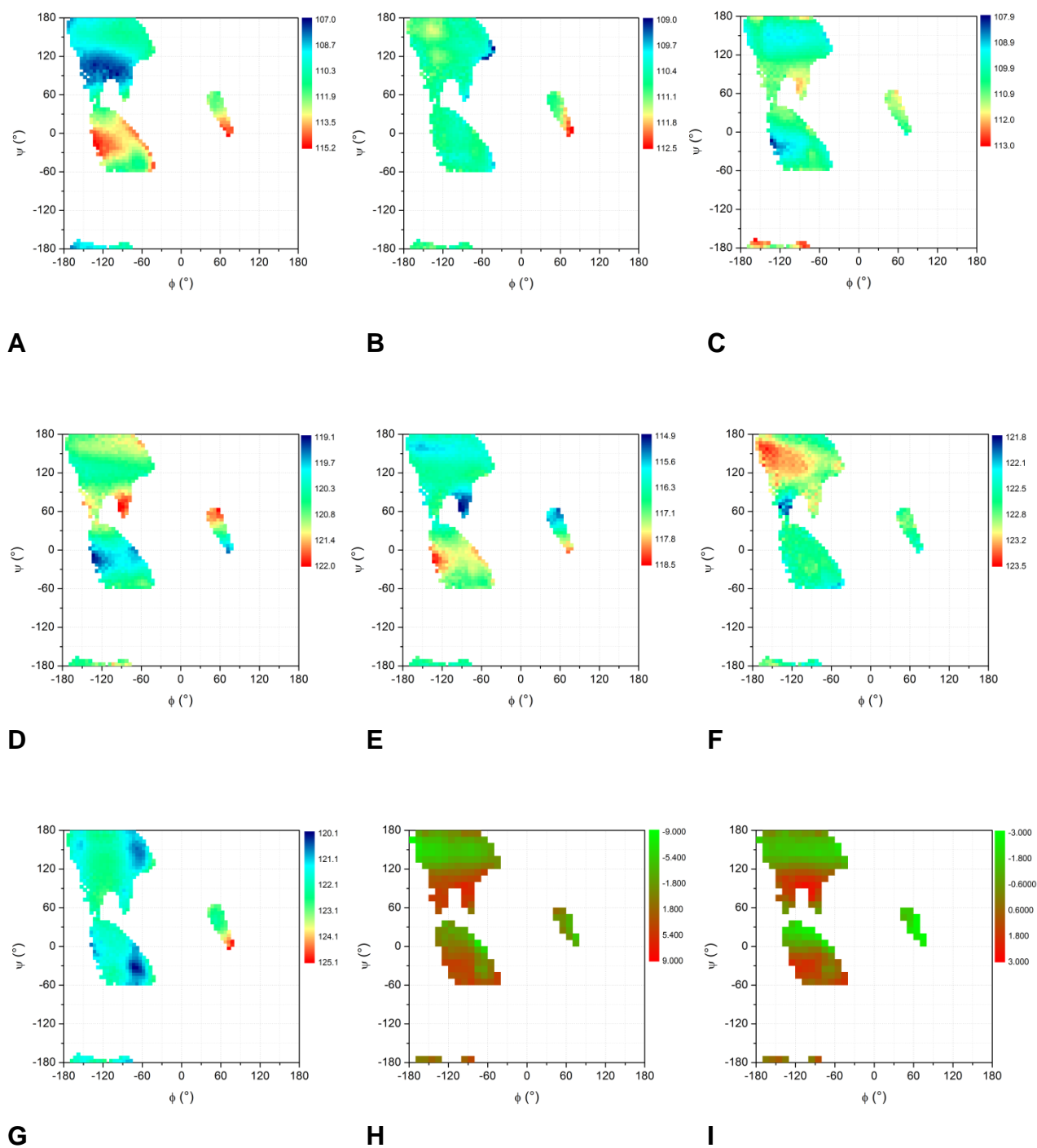
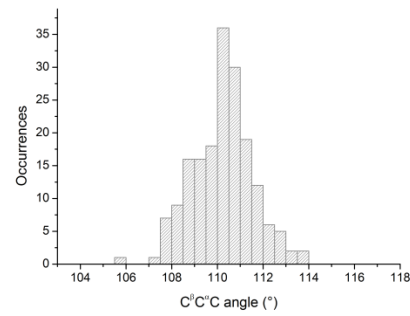
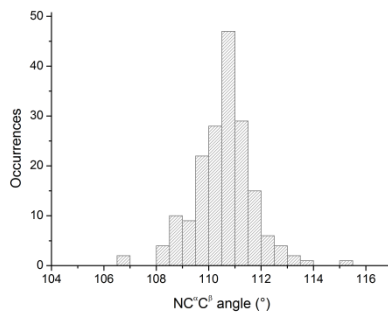
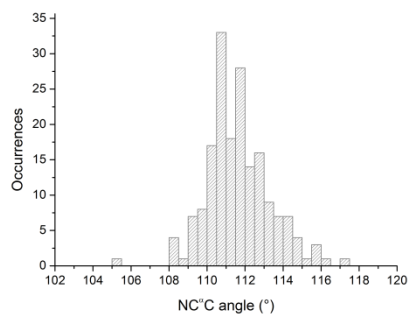
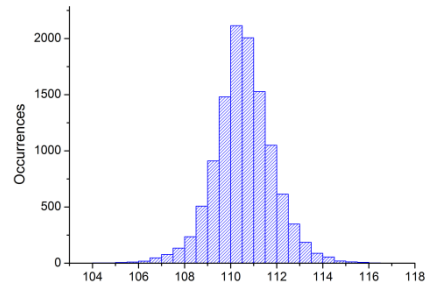
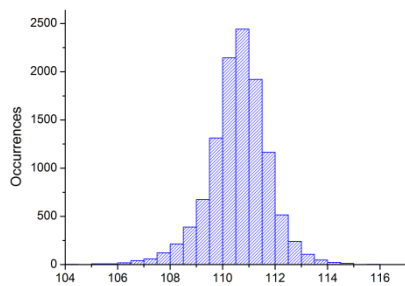
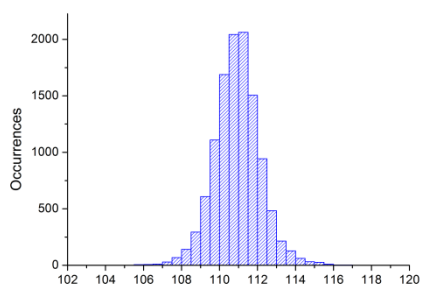


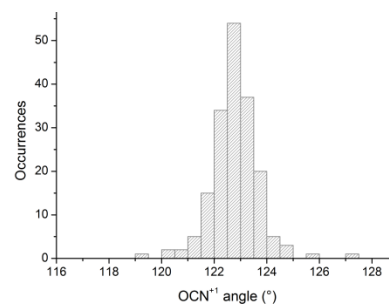
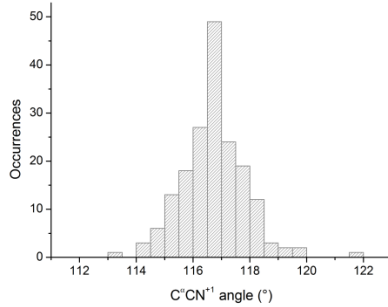
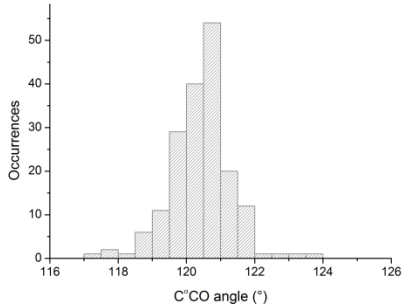
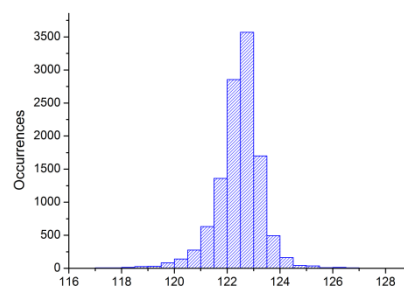
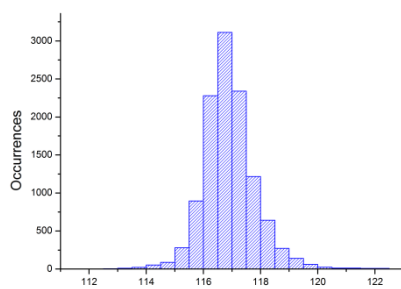
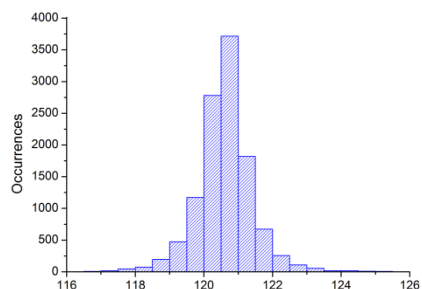
Figure S1. Ramachandran plots highlighting the experimental dependence of the bond angles $NC^{\alpha}C^{\beta}$ (A), $NC^{\alpha}C^{\beta}$ (B), $C^{\beta}C^{\alpha}C$ (C), $C^{\alpha}CO$ (D), $C^{\alpha}CN^{+1}$ (E), OCN^{+1} (F), $C^{-1}NC^{\alpha}$ (G) and dihedral angles $\Delta\omega$ (H), θ_C (I) on backbone conformation (ϕ , ψ) for the eighteen non-Gly/non-Pro residues. The mean values are calculated in $5^{\circ}\times 5^{\circ}$ and $10^{\circ}\times 10^{\circ}$ (ϕ , ψ)-boxes for bond and dihedral angles, respectively. Only boxes containing at least 50 residues were considered.



A

B

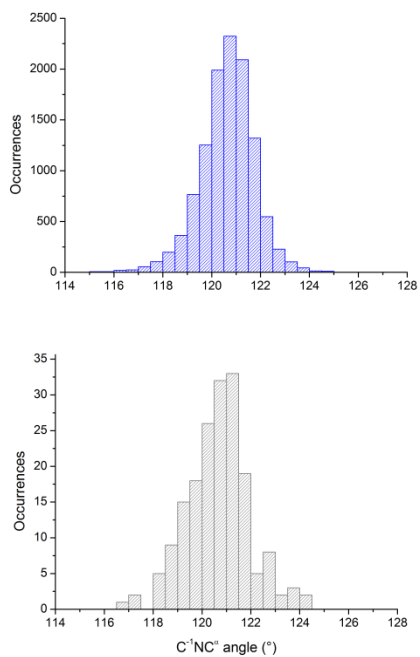
C



D

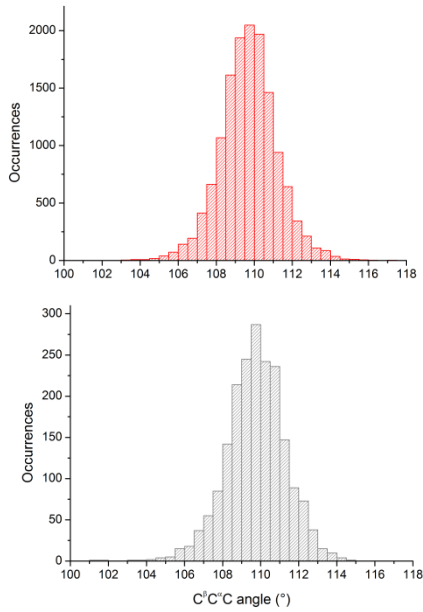
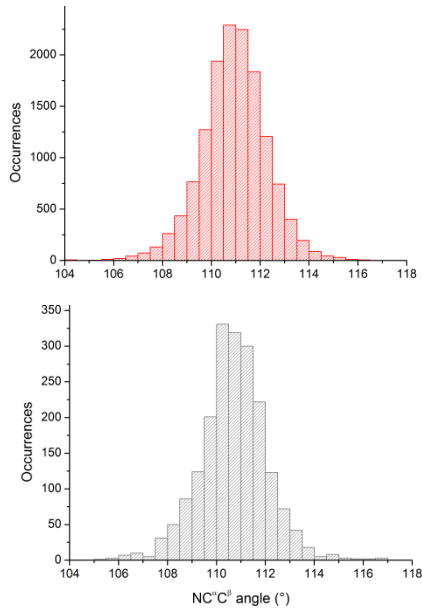
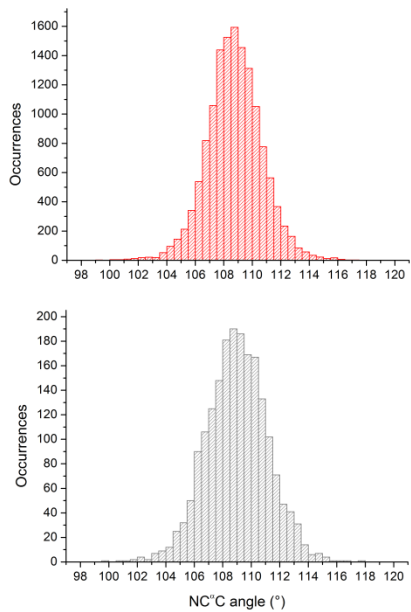
E

F



G

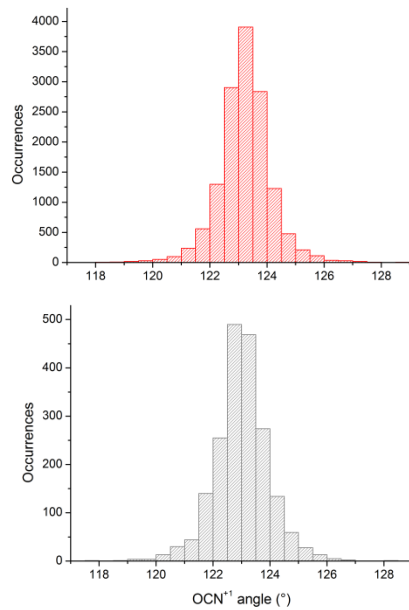
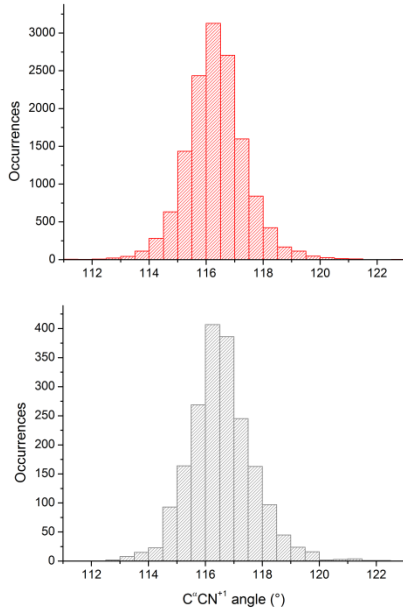
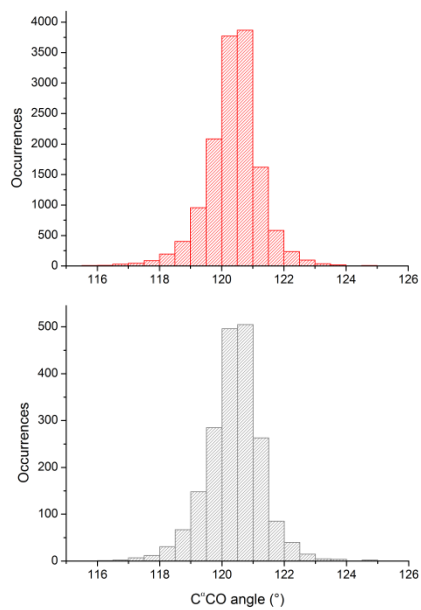
Figure S2. Distributions of bond angles values of non-Gly/non-Pro residues in α -helix (blue) or coil (grey) in the $3^\circ \times 3^\circ$ -box centered at $(\phi, \psi) = (-63^\circ, -43^\circ)$: $NC^\alpha C$ (A), $NC^\alpha C^\beta$ (B), $C^\beta C^\alpha C$ (C), $C^\alpha CO$ (D), $C^\alpha CN^{+1}$ (E), OCN^{+1} (F), $C^{-1}NC^\alpha$ (G).



A

B

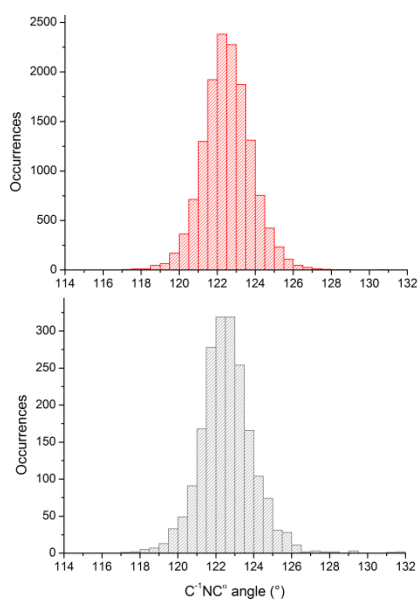
C



D

E

F



G

Figure S3. Distributions of bond angles values of non-Gly/non-Pro residues in β -sheet (red) or coil (grey) in the $15^\circ \times 15^\circ$ -box centered at $(\varphi, \psi) = (-120^\circ, 130^\circ)$: NC^αC (A), $\text{NC}^\alpha\text{C}^\beta$ (B), $\text{C}^\beta\text{C}^\alpha\text{C}$ (C), C^αCO (D), $\text{C}^\alpha\text{CN}^{+1}$ (E), OCN^{+1} (F), $\text{C}^{-1}\text{NC}^\alpha$ (G).